BRAIN CONNECTIVITY
Volume 1, Number 4, 2011

DOI: 10.1089/brain.2011.0036

A Sliding Time-Window ICA Reveals Spatial Variability of the Default Mode Network in Time

Vesa Kiviniemi, Tapani Vire, Jukka Remes, Ahmed Abou Elseoud, Tuomo Starck, Osmo Tervonen, and Juha Nikkinen

Abstract

Recent evidence on resting-state networks in functional (connectivity) magnetic resonance imaging (fcMRI) suggests that there may be significant spatial variability of activity foci over time. This study used a sliding time window approach with the spatial domain–independent component analysis (SliTICA) to detect spatial maps of resting-state networks over time. The study hypothesis was that the spatial distribution of a functionally connected network would present marked variability over time. The spatial stability of successive sliding-window maps of the default mode network (DMN) from fcMRI data of 12 participants imaged in the resting state was analyzed. Control measures support previous findings on the stability of independent component analysis in measuring sliding-window sources accurately. The spatial similarity of successive DMN maps varied over time at low frequencies and presented a 1/f power spectral pattern. SliTICA maps show marked temporal variation within the DMN; a single voxel was detected inside a group DMN map in maximally 82% of time windows. Mapping of incidental connectivity reveals centrifugally increasing connectivity to the brain cortex outside the DMN core areas. In conclusion, SliTICA shows marked spatial variance of DMN activity in time, which may offer a more comprehensive measurement of the overall functional activity of a network.

Key words: functional connectivity; functional (connectivity) magnetic resonance imaging; independent component analysis; resting-state sliding window; spatial stability

Analysis of spontaneous fluctuations in brain activity in the absence of tasks (i.e., in the "resting state") has grown to be an effective tool in the evaluation of baseline brain activity and functional connectivity (Biswal et al., 1995; Biswal 2010). Although initially the connectivity may have been assumed to be stationary, fairly recently it was noticed that the connectivity between functional regions is not by any means stable; rather, measures of functional connectivity oscillate considerably over time (Chang and Glover, 2010). Correlation coefficients between two connected brain regions can vary from nearly +1 to −1 as a function of time. Active brain loci can be phase locked, negatively correlated, or even in orthogonal phases in their oscillation activity with respect to each other.

Repeatability studies on brain activation also show considerable spatial variability in addition to temporal variability. Regional task-related brain activity shows extensive variability in both interindividual and intraindividual comparisons (Birn et al., 2001, Fernandez et al., 2003; Neumann et al., 2003; Rombouts et al., 1998; Saad et al., 2003; Salli et al., 2001; Tjandra et al., 2005; van Gelderen et al., 2005; Yoo et al., 2007). The intraindividual spatial variability of brain activity has been related to low-frequency physiologic effects (Birn et al., 2001; Kannurpatti et al., 2008; Kannurpatti et al., 2011; Mennes et al., 2010; Mennes et al., 2011; Saad et al., 2003).

Spatial domain independent component analysis (ICA) can robustly detect resting state networks (RSNs) (Biswal et al., 2010; Beckmann et al., 2005; Damoiseaux et al., 2006; Greicius 2004; Long et al., 2008). However, after increases in the model order, ICA has been shown to give more parceled spontaneous activity loci within networks (Abou Elseoud 2010; Kiviniemi et al., 2009; Smith et al., 2009). This is possible because of better coverage of the total data variance with higher model orders, especially in group data. New multilevel bootstrap analysis of stable clusters reveals marked stability variations in RSNs both within and between individuals (Bellec et al., 2011). The stability of the RSN clustering seems to be good in primary somatosensory cortices, but frontoparietal RSNs present clearly less stable connectivity matrices.

Department of Diagnostic Radiology, Oulu University Hospital, Finland.

The brain functions and their connectivity may be spatially less restricted in time during the resting state. One of the most dominant resting-state networks, the default mode network (DMN), in particular has been related to a multitude of different functions often targeted toward the monitoring of several functions, such as inner milieu, attention, and memory (Buckner 2008; Fox et al., 2005; Fox and Raichle 2007; Raichle et al., 2001). Because the DMN has independent subregions in high model order studies and because it has marked time-frequency variability, the DMN network may not be stable spatially over time, but its subnetworks may present marked variability in time. The study hypothesis was that the spatial distribution of DMN network activity varies significantly over time. This hypothesis was tested by measuring spatial stability of the DMN maps obtained as a function of time. Spatial independent component analysis was modified with a sliding temporal window ICA (SliTICA) approach to obtain information about the spatial behavior of the DMN as a function of time.

Methods

The Ethical Committee of Oulu University Hospital, Finland, approved the study. Twelve healthy participants, who all gave written informed consent (six men; mean age, 29.9 years [range, 24–48 years]) were scanned with a GE Signa HDx 1.5-T whole-body system with an eight-channel receiver coil. Motion was minimized by using soft pads fitted over the ears, and hearing was protected. The session started with a T1-weighted three-dimensional fast spoiled gradient recalled (FSPGR) sequence (repetition time [TR], 12.1 msec; echo time [TE], 5.2 msec; slice thickness, 1.0 mm; field of view, 24.0 cm; matrix, 256 × 256; and flip angle, 20°) to obtain anatomical images for co-registration of the functional magnetic resonance imaging (fMRI) data to standard space coordinates. After the anatomical scans, resting-state blood oxygen level–dependent (BOLD) data were collected by using an echo planar imaging gradient recalled echo sequence (TR, 1800 msec; TE, 40 msec; 280 time points; 28 oblique axial slices; slice thickness, 4 mm; interslice space, 0.4; whole brain coverage; field of view, 25.6 × 25.6 cm; matrix, 64 × 64; parallel imaging factor, 2; and flip angle, 90°). Participants were simply told to stay still and rest with their gaze fixed on a cross shown via mirrors onto a screen.

Data preprocessing

The BOLD data were preprocessed with a typical FSL (FMRIB, Oxford, United Kingdom)-preprocessing pipeline as described elsewhere (Abou Elseoud 2010; Kiviniemi et al., 2009). Head motion was corrected by using motion correction linear image registration tool software (Jenkinson et al., 2002), and brain extraction was performed (Smith 2002) with parameters f = 0.5 and g = 0; for three-dimensional fast spoiled gradient recalled, f = 0.25 and g = 0 were used. The BOLD volumes were smoothed with a Gaussian kernel of 5 mm full width at half maximum, and time series were high-pass–filtered by using a 120-sec cutoff with an fslmaths tool. Multiresolution affine co-registration within FSL 4.1.4 linear image registration tool software (Jenkinson et al., 2002) was used to co-register mean, nonsmoothed fMRI volumes to three-dimensional FSPGR volumes of corresponding participants, and to co-register three-dimensional FSPGR volumes to the Montreal Neurological Institute (MNI) standard structural space template.

ICA analysis

ICA analysis was carried out using FSL 4.1.4 MELODIC software implementing probabilistic ICA (PICA) (Beckmann and Smith, 2004). The single-subject PICA (implementing a FastICA algorithm) was performed in two ways: 1) with a conventional whole time series (wtsICA) consisting of all 250 brain volumes imaged and 2) with SliTICA. The time-domain signals were variance-normalized, and automatic dimensionality estimation was used with default settings. Finally, a group PICA analysis, using dimensionality estimation, was also performed for comparison with individual ICA decompositions.

Pioneering ICA research teams have shown that the sliding-window approach detects robust activation results even for real-time feedback of activity (Esposito et al., 2003; Karvanen and Theis, 2004). SliTICA was performed by cropping the original 250 time point BOLD data set into time windows of 60 time points and sliding the 60 volume time window one volume at a time: 0–59, 1–60, 2–61,…, 190–249 (Esposito et al., 2003; Karvanen and Theis, 2004). This procedure yielded 190 time windows in total. All data were analyzed with PICA using model order estimation. The resulting IC source maps were thresholded using an alternative hypothesis test based on fitting a Gaussian/gamma mixed model to the distribution of voxel intensities within spatial maps (Beckmann and Smith, 2004; Beckmann et al., 2005) and controlling the local false-discovery rate at a $P < 0.5$.

The DMN source was identified from the whole time series wtsICA using criteria identical to those previously reported, with low frequency fluctuation in the IC signal in the posterior cingulate cortex, the angular gyri bilaterally, and the ventromedial prefrontal cortex (Abou Elseoud et al., 2010; Greicius et al., 2004; Kiviniemi et al., 2009; Smith et al., 2009). The identified default mode IC from wtsICA was then used as a spatial template against which successive maps of the default mode were identified from the successive 190 SliTICAs. The identification was based on two spatial measures: in the first step the spatial similarity was calculated by the correlation coefficient between the wtsICA DMN template and successive SliTICA ICs with FSL's spatial correlation analysis tool fslcc. The second step was visual verification of the SliTICA signal sources as a DMN source; there the emphasis was laid on the typical appearance of the DMN nodes and low frequency fluctuations in the IC signal. If two or more similar or unclear IC sources were detected, then the higher correlation value (more similar to the template wtsICA source) was primarily chosen.

Spatial analysis of SliTICA

The spatial stability of the DMN was analyzed as a function of time by measuring a spatial correlation of the detected DMN SliTICA sources using fslcc. The stability measures were performed in two ways by comparing 1) a commonly used wtsICA DMN template from every individual and 2) the first and last SliTICA source to the rest of the successive SliTICA DMN maps. This yielded a time domain signal of the spatial stability over the 190 windows. A phase and power spectrum of the spatial stability was calculated by

using OriginPro 8 (OriginLab Corp, Massachusetts) to obtain group-level estimates of the frequencies involved in spatial stability changes from the wtsICA comparison. The SliTICA maps were calculated in three ways: 1) mean z-score and 2) standard deviation of z-score maps over time, and 3) a cumulative map over all the 190 time windows of voxels (threshold $|Z| > 2.3$) was counted with fslmaths and referred to as the cumulative incidence map. Individual maps were spatially registered to 2 mm MNI 152 T1-weighted images and summed into a group map showing general trends in the spatial pattern of the DMN over the 190 time windows. In addition, successive SliTICA maps of each individual were fused into DMN videos of the whole group over the 190 windows. The group mean z-score maps reveal DMN activity as a function of time and space. Also, the explained variance percentage of the chosen IC was calculated with respect to the windows' own variance and total data variance.

Performance measurements of the SliTICA

The sliding-window ICA has been successfully verified by two pioneering ICA research groups for activation studies (Esposito et al., 2003; Karvanen and Theis, 2004). Sliding-window ICA has not been applied to resting-state studies, which do not have clearly controllable timing of detectable events. The spatial form or strength of a given source within the data may be unclear. The stability of the SliTICA approach was therefore estimated for the resting state in two ways. The first was to measure the variability of the sliding BOLD data windows with dimensionality estimation (default setting) in PICA, by which means model order was obtained as a function of the sliding-window point. The other way estimated the spatial stability of successive SliTICA maps on a glitch artifact detectable in the wtsICA in one slice of the BOLD data. The glitch is an occasionally occurring short-term electronic fault of the scanner and leads to a false formation of image k-space data in one or a few slices. As a technical problem it is separate from physiologic signal sources in the BOLD data but shares some of the noise properties of the scanner system and is clearly an independent source within the data. The glitch artifact was considered a data-derived model to test the sensitivity of the SliTICA method.

Results

As a control measure, a single slice glitch artifact was measured as a function of time. The artifact occurred as an independent component in the wtsICA and is present exactly in those data points within the 60 time points long SliTICA window frame in Figure 1. The glitch artifact remained spatially stable over the whole 60-point SliTICA time range when compared with the wtsICA glitch map. When the data window was outside the point in time of the glitch artifact (73rd scan), no artifact images were found and the best fit spatial correlation coefficient falls to a noise level around 0.1. The spatial correlation of the detected glitch artifact within the SliTICA time window stays within a narrow range at 0.3 correlation coefficient and fluctuates considerably less compared with the DMN fluctuations described next (Fig. 2).

The model order estimated by PICA from successive sliding windows shows that it remains relatively stable over time, the mean value being around 15 (range, 13–19; Fig.1, middle). There is no clear variability in the successive windows at the mean or individual levels, and therefore the model order of the SliTICA is also not a factor that affects the DMN maps. On average, each DMN IC explained 6.7% ± 0.3% of the windows' data variance and 4.0% ± 0.17% of the total data variance. The explained variance of the DMN IC did not alter as a function of time (result not shown).

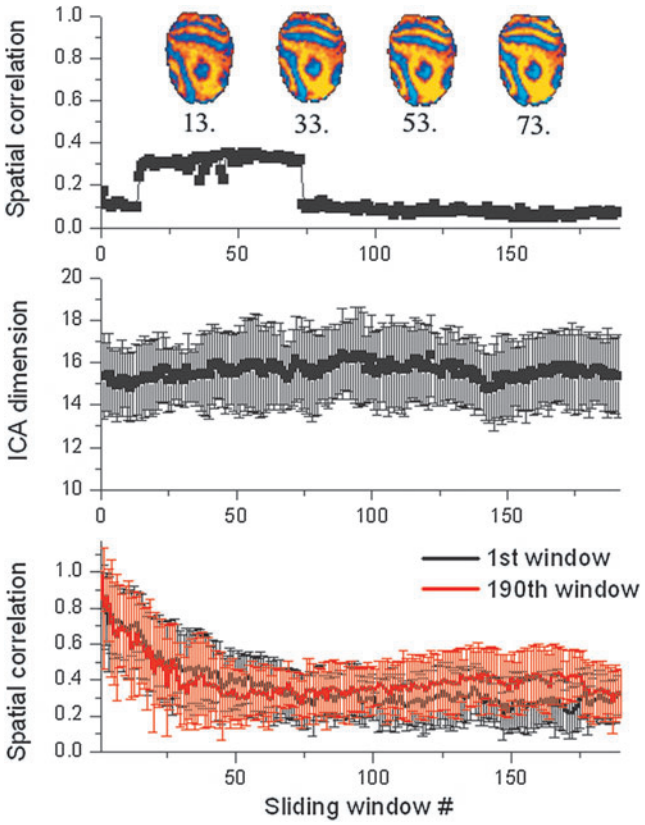

FIG. 1. **(Top)** Spatial similarity of the glitch artifact as a function of sliding window number shows the presence of the independent glitch artifact as detected by the whole time series independent component analysis (ICA) compared with sliding time window ICA (SliTICA). The true correlation is at 0.3 measured with fslcc from z-score maps without binarizing. Examples of the glitch are shown on top of the curve with corresponding time window number beneath. **(Middle)** The number of estimated independent components as a function of sliding-window number presents a stable mean model order around 15 independent components (range, 13–19). **(Bottom)** Spatial correlation coefficient with fslcc of successive SliTICA default mode network (DMN) maps compared with the first (black) and last (red) sliding window as a function of window number reveals exponential decay in DMN spatial similarity from the beginning of the scan. The last red window similarity curve is temporally reversed for easier comparability with the first black curve.

Spatial stability of the DMN

There is an exponential decay in the spatial stability of the DMN over time when compared with the first DMN map obtained from the sliding window of images (0–59; Fig. 1, bottom). The average spatial similarity starts from around 0.8 and diminishes exponentially for around 60 time points

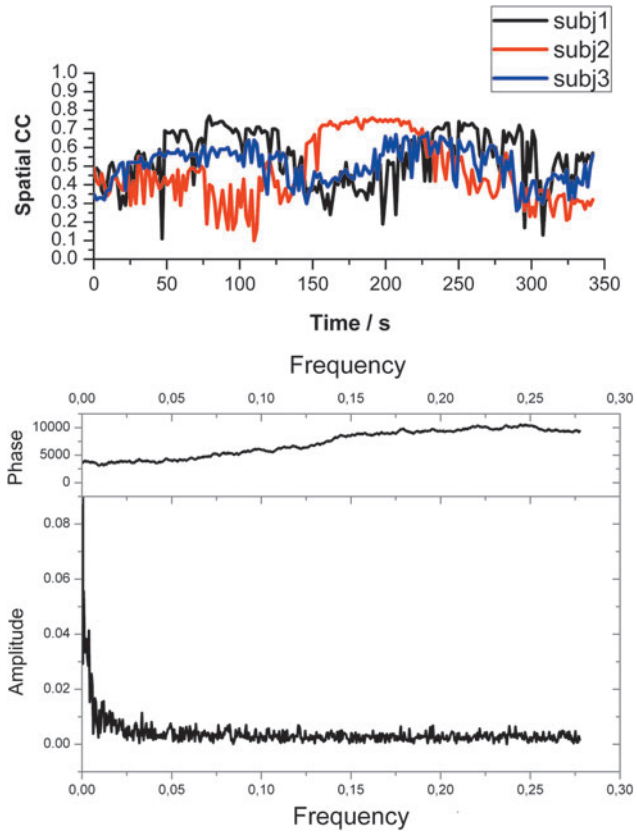

FIG. 2. **(Top)** Three participants' measured spatial stability in comparison to the default mode network whole time series independent component analysis (wtsICA) template over time shows low frequency fluctuation. **(Bottom)** Phase and mean fast Fourier transform power spectrum of the 12-subject spatial correlation coefficient (CC) over 190 time windows reveals 1/f behavior of the spatial stability measure compared to the wtsICA template.

before reaching a baseline similarity at around a level of 0.3. Nearly identical decay can be detected in reverse when successive images are compared to the last scan.

The spatial stability of DMN in SliTICA presented a low frequency fluctuation over time. Three examples of time domain evolvement of spatial similarity between the wtsICA and successive window images are shown in Figure 2 (top); a fourth participant is shown in Figure 3 (bottom) with representative network activity overlaid on individual T1-weighted images. The fluctuation detected in individual SliTICAs compared to wtsICA differs between participants and is not phase locked. The power spectrum of the spatial stability reveals 1/f behavior in the similarity of the spatial pattern of a DMN over time (Fig. 2, bottom).

Figure 3 presents examples of classic wtsICA maps and SliTICA maps with respect to the detected spatial similarity values over time. The commonly used wtsICA maps themselves seem to originate from relatively sparse periods of time during the whole scan and therefore may not resemble the classic DMN perfectly (see also Fig. 3). The successive SliTICA maps reveal spatial migration of independent DMN activity within the classic DMN nodes, literally back and forth in time. Intriguingly, there also appears to be incidental connectivity foci outside the DMN nodes. These short-lived connections cover a considerable area of the brain that grows centrifugally from the nodes when more maps are fused into a cumulative incidence map. The DMN activity itself shows a centripetal incidence pattern in total image incidence and averaged maps.

Mapping spatiotemporal variability

Mean group solicit maps shown as a function of time present the evolution of the DMN mean z-score over time within the whole group on a voxel-by-voxel basis. Based on previous literature, there should not be any temporal patterns in the mean solicit z-score maps; rather, the z-score should be fairly random (Chang and Glover, 2010). However, the z-score time signals of the group map are not stable lines, nor are they similar in different nodes. An example voxel (Fig. 4) from the posterior cingulate cortex of the detected DMN maps presents a wide group mean z-score elevation after the onset of scanning while the ventromedial prefrontal cortex shows a sharper and shorter elevation of group mean z-scores, which declines out quickly. Notably, the bilateral activity at parietal regions near angular gyri presents a markedly different flattened temporal pattern with a lower group mean z-score as well, especially on the right side (Fig. 4).

An attempt to condense the spatial variability can be seen in the cumulative incidence group map. There, large portions of the brain cortex are incidentally connected to the DMN at least a few times within the 190-image timeframe. However, the Rolandic areas and some basal cerebral and cerebellar regions do not pass the threshold in any of the scans. After setting a threshold with $|Z| > 2.3$, there is a striking finding in the summed group incidence map; no single voxel among the 12 participants was connected to the DMN in each of the 190 sliding windows, not even inside the highest mean z-score areas within the DMN core areas of the posterior cingulate cortex or ventromedial prefrontal cortex. The activity focus shifts so much that the maximum number is 155 out of the possible 190 (i.e., in standard MNI space, best-fit DMN-independent activity is present maximally in 82% of windows [Fig. 4]). This finding shows that DMN activity varied spatially even among the core areas of the DMN over time. The standard deviation map of z-scores showed the most marked variation occurring in areas near the frontal and occipital edges of the brain and these overlap partly with the core areas of the DMN. These areas are in the posterior parts of the parietal DMN sources and were predominantly left sided.

Discussion

Sliding time window spatial ICA can detect clear, low-frequency variability in the spatial distribution of default mode RSNs over time in a similar fashion to fluctuating connectivity patterns detected by Chang and Glover (2009). The spatial similarity of successive DMN maps fluctuated markedly on low frequencies and showed a power spectral 1/f frequency distribution (Fig. 2). Importantly, the independent brain activity of the DMN migrates considerably both within the DMN nodes with short-lived connectivity scatters outside the classic DMN nodes. The core activity of the functional nodes is centripetal in nature, whereas incidental connectivity grows centrifugally. The cumulative incidence map of the whole 12-participant group also shows that suprathreshold voxels ($|Z| > 2.3$) were present in only maximally 82% of

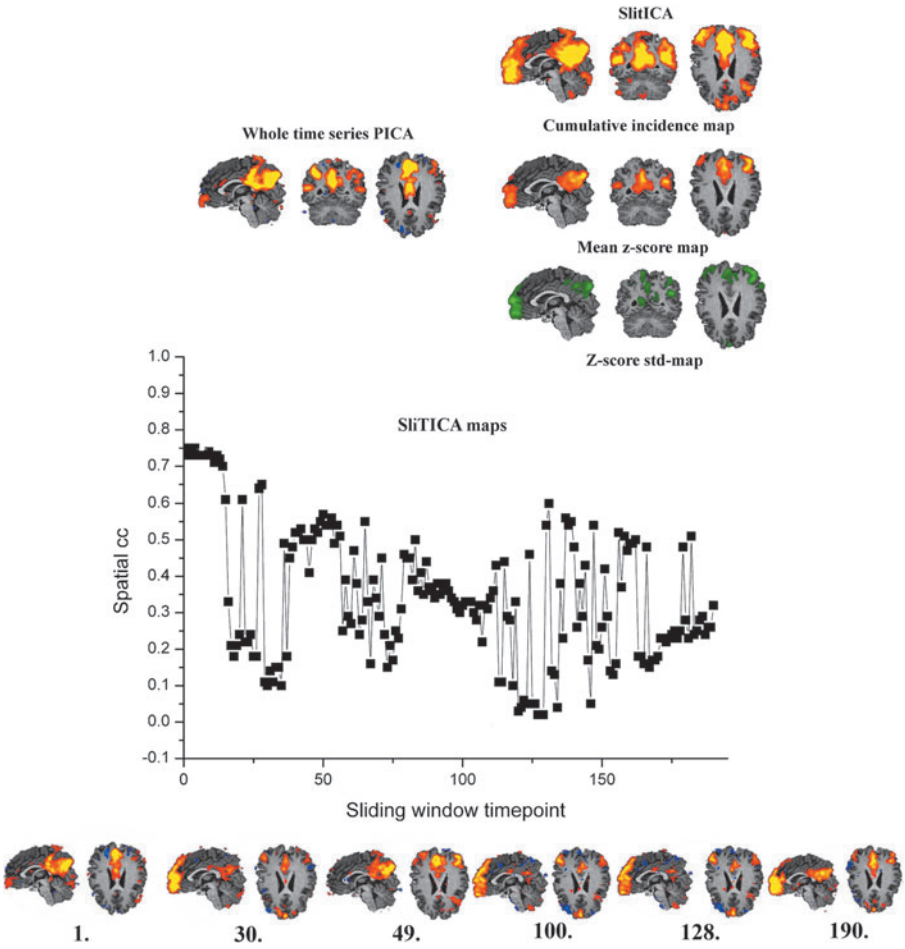

FIG. 3. **(Top)** A single-subject whole time series independent component analysis (wtsICA) is shown on the top right with the same participant's cumulative incidence, mean z-score, and standard deviation maps for comparison on the left. **(Bottom)** In the spatial similarity plotted as a function of window number shows that the spatial similarity compared to the wtsICA fluctuates markedly over time, which can be seen from the curve below. Window images portraying minimal and maximal local spatial correlation coefficients (CCs) are shown for visual comparison, with corresponding window numbers beneath. PICA, probabilistic independent component analysis; SliTICA, sliding time window independent component analysis.

time windows. This finding suggests that no single brain area or even a voxel is continuously connected to one single default mode network activity but rather the activity captured by BOLD data is spatially heterogeneous in time.

Momentary interactions of segregated activity loci

According to Friston, a single brain function may involve many specialized brain areas whose union is mediated by the functional integration among them (Friston 2011). Small-world network analyses on brain functional connectivity support the integration of widespread activity units with relatively few inter-unitary hubs (Achard et al., 2006). On the same note, a recent meta-analysis showed that brain activity from over 1600 brain activation studies could be explained by 45 independent brain networks (Smith et al., 2009). Markedly similar networks are also active in the resting state with ICA (Kiviniemi et al., 2009; Smith et al., 2009).

The RSNs can be fractioned into several subunits because of the increased sensitivity of high model order ICA in detecting different spatial distributions of activity (Abou Elseoud 2010; Kiviniemi et al. 2009; Smith et al., 2009). However, splitting RSNs robustly into identifiable subunits has not been possible from single-subject data, typically measured over the whole time series. This could be due to the detection of sparse events, temporal averaging, or the fact that the PCA step used in ICA depicts only the subfunctions that produce most variance over the whole time and may miss subtle differences in the signal.

SliTICA, on the other hand, can reflect how multiple different default state subfunctions present themselves independently in space through time even in a single-subject measurement. The PCA dimension reduction step used in ICA may be more tuned toward subtle and more temporary activities within the sliding window. The ICA algorithms have the mathematical tendency to emphasize sparsity (Daubechies et al., 2009). The results of this study are in agreement over this issue. It seems that the spatial ICA methods may (also) emphasize temporally sparse events with the highest spatial independence in time. Relatively few time windows have high spatial correlation between the best fit maps in Figures 2 and 3. Importantly, the sliding-window approach at least partly overcomes the bias toward temporal sparsity by forcing the algorithm to search for more subtle sources from within a narrowed window. Thus, SliTICA can detect weaker or incidental connections beneath the stronger sources that dominate over longer time periods in wtsICA.

Interestingly, negative values (i.e., reverse/anticorrelation) are also picked up (Fig. 3). That is nonstationary. This is important because global signal regression was not performed and the anticorrelations seem real and not mathematically induced. It is important to notice that because ICA rotates data freely, the adverse effects of global signal regression around the mean value are not so prominent. The study by Chang and Glover (2009) also seems to point toward nonstationary processes in anticorrelations as well.

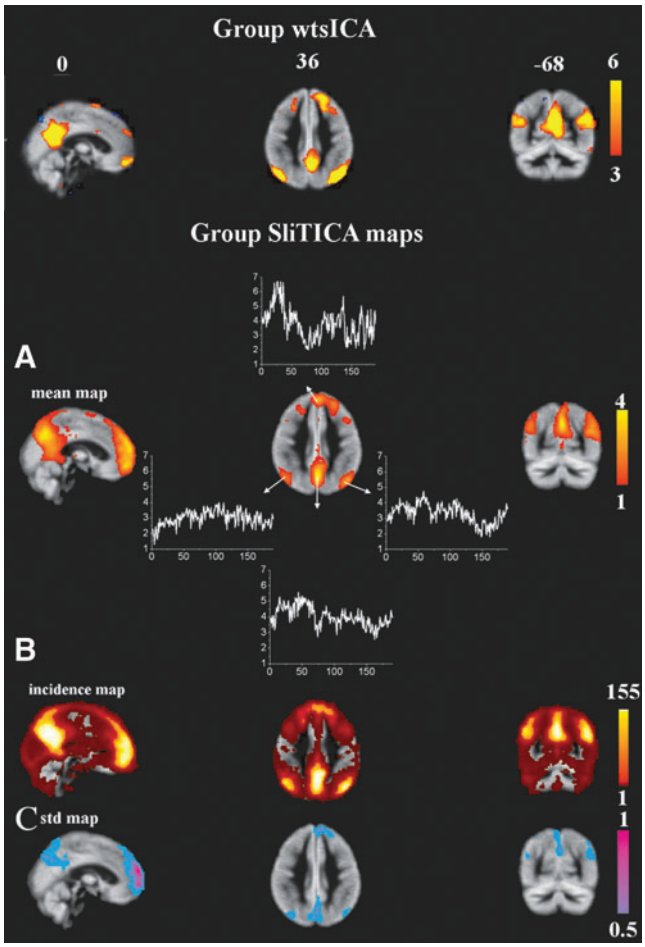

FIG. 4. **(Top)** Classic group probabilistic independent component analysis of all participants. **(Bottom)** Sliding time window independent component analysis (SliTICA) results: Mean z-score map of all 190 SliTICA default mode network maps reveals marked z-score value variability as a function of window. In particular, the bilateral angular gyri are markedly dissimilar to ventromedial prefrontal cortex or posterior cingulate cortex areas. **(A)** A mean z-score time course of a voxel from each area is presented in white. **(B)** Cumulative incidence map of voxels having $|Z| > 2.3$ threshold in the 190 windows. The maximum is only 155 in any of the voxels. **(C)** Standard deviation (std) of the z-score maps over all the sliding windows. Color bars on the right show the range of color encoding in the image. wtsICA, whole time series independent component analysis.

Spatial extent of functional connectivity

Data from repetitive scans of brain activation show that after averaging 22 scans an increase in the supra-threshold activation volume up to a factor of 13 can be achieved (Saad et al., 2003). When one increases the number of repetitions, the activity seems to spread centrifugally from the most robust nodes of activity. The cumulative SliTICA incidence maps of this study show very similar centrifugal spread as a function of incidence number. In other words, both activation and resting-state activity convey very similar increases in the volume of brain activity with repetitive mapping. The DMN performs multiple tasks and collects information from multiple sources around the brain with different activity (Buckner 2008; Fox and Raichle 2007; Raichle, et al. 2001). Our finding of centrifugally growing incidental connections outside the DMN core regions can be regarded as a sign of occasional functional cross-talk of a DMN to other brain regions.

Increasing evidence suggests that the variability of brain activation data may be related to low-frequency physiological phenomena of the brain, such as cardiorespiratory undulations, vasomotor waves, neuronal oscillations, and metabolic fluctuations (Kannurpatti et al., 2008; Kannurpatti et al., 2011; Mennes et al., 2010; Mennes et al., 2011; Saad et al., 2003). The low-frequency spatio-temporal variance captured by the sliding-window ICA approach in this study may be related to the very same physiological effects. When compared with whole time series ICA, SliTICA detects low-frequency fluctuations at spatial similarity values in the same frequency range as those earlier detected in the connectivity measures. Interestingly, the power spectrum of the spatial similarity measure also reveals a $1/f$ nature. The $1/f$ behavior is a sign of a natural phenomenon that is fractal, as many things in nature are. This suggests that spatial variation of independent DMN activity in time has long-term memory in its processes (i.e., when the spatial patterns present repeating elements in multiple time scales).

Spatial boundaries vs. variance

Other parcellation methods have been able to separate the brain areas into multiple functional nodes as well (Bellec et al., 2010; Cohen et al., 2008; Yan et al., 2011). The boundaries of those nodes have been shown to predict subject performance and task activation (Mennes et al., 2010; Mennes et al., 2011). It is interesting that both in repeatability analyses of brain activity and in the SliTICA results of this study, the spatial variability/low connectivity incidence is most marked on the boundaries of the active network. Regional homogeneity and BOLD signal amplitude is also highest within the DMN core areas, including the posterior cingulate cortex and ventromedial prefrontal cortex, and they decrease toward external boundaries (Biswal et al., 2010; Long et al., 2008).

Boundaries between default mode and task-positive networks overlap with the frontoparietal network that controls and monitors brain activity with DMN (Mennes et al., 2011). The largest spatial variability with low incidence of functional connectivity is located at the edges of the DMN as well (Fig. 4). The boundaries between the most robust activity centers of both strong functional connectivity and brain activation seem to be a functional "no-man's-land." Boundaries may serve as areas belonging to no specific task but rather could be seen as interfunctional processing areas. Interestingly, as such they are detected in group PICA analyses as independent sources (Kiviniemi et al., 2009; Smith et al., 2009). An interesting new connected iterative scan mapping method seems to be able to incorporate such information into an adaptive analysis of the data (Yan et al., 2011). It remains to be seen whether the detected short-term variance in connectivity at boundaries is related to functional cross-talk between network nodes.

Implications of DMN spatio-temporal variability

Most other functional connectivity approaches use measures of time domain connectivity, which are likely to suffer

from limited temporal sampling resolution of fMRI in the second range unless hours of scanning per subject are performed with the present methods (Smith et al., 2010). SliTICA offers much detailed information about a brain network as a statistical measure in the spatial domain rather than time domain. As such, the method could also be seen as a way to increase the amount of information for statistical analyses of one single scan because averaging over time is minimized. In this sense SliTICA may be used as a way to increase statistical power for disease detectability, fcMRI is rapidly approaching diagnostic accuracy (Fox and Greicius 2010; Greicius et al., 2004; Greicius et al., 2008). SliTICA may be used as a way to increase statistical power in order to increase sensitivity to disease related changes. In diagnostics, the single-subject-level analysis is mandatory; on the basis of the current results, however, a much more comprehensive analysis could be obtained by using the SliTICA approach instead of classic wtsICA.

WtsICA seems to prefer temporal sparse activity patterns by taking only a few temporal events into account. This does not always produce a very comprehensive spatial activity pattern at the single-subject level (Fig. 3). Using incidence maps as a cumulative measure could augment the clinical differentiation capability by detecting the related areas of activity more comprehensively. In addition, ICA separates noise sources and seems not to be so sensitive to global mean regression problematics or noise due to angle-free statistical analysis of the data distributions. The sliding-window approach may reflect cortical neurophysiology more comprehensively by portraying rich moment-to-moment variability. Therefore the occasional connectivity scatters may actually be very fruitful for diagnostics. The most important improvement is the increase in sensitivity over the common wtsICA approach.

In the same vein, the anatomical selection of the region of interest used to derive reference time courses in classic correlation analyses may be influenced by the spatial variance of the ongoing brain activity. It was recently shown that region-of-interest selection alters functional connectivity results and that data-driven individual results outperform other measures (Marellec and Fransson, 2011). The results of Marellec and Fransson are in excellent accordance with the current results. If the core baseline brain function or guided task process spatially shifts away from the region of interest, then brain activity measures such as functional connectivity values can alter in unexpected ways. One such unexpected result could be the incidental orthogonal correlation values in wavelet-based connectivity analyses with sliding-time windows (Chang and Glover 2010). Data-driven methods sensitive to the spatial stability changes occurring over time are supported in the selection of regions of interest for functional connectivity analyses.

Auto-correlation of successive-window DMN

There was an invariant exponential drop in the spatial similarity of the DMN as a function of time from the beginning resting-state scan. This was first thought to be a physiological sign of loss of interest within the DMN on the visual fixation. However, after further analysis a near-identical decay could be identified in reverse when SliTICA maps were compared to the last window. This autocorrelation type pattern may be related to the overlap between a large portion (59/60) of the data from successive windows. Shorter windows and less overlap between successive windows might increase the sensitivity to even faster spatial alterations. The comparisons to wtsICA show slow fluctuations but also more rapid alterations in correlation can be detected. The rapid changes in similarity were often correlated to the emergence of two or three nearly similar patterns of DMN, which were not further analyzed in this study.

Technical issues

The sliding-window ICA approach is not completely new; it has been introduced to fMRI activation studies before. The SliTICA approach uses the abundant spatial domain information in detecting independent BOLD signal sources as a function of time (Beckmann et al., 2004; Calhoun et al., 2001; Greicius 2004; Kiviniemi et al., 2003; McKeown et al., 1998). A comprehensive pioneering work by Esposito and colleagues (2003) showed that the fast ICA developed by Hyvärinen (1999) can meet the requirement for fast processing required in real-time fMRI analysis by the sliding time window approach with good accuracy. They suggested that theoretically even two successive brain volumes could render enough information for spatial ICA to depict targeted activity. However, they preferred to use 10 images as a window. Karvanen and Theis (2004) showed marked spatial variability in their auditory cortex study using a 20 time point window length.

In this study, a significantly longer 60 time point window was chosen; this window has been used in earlier studies to cover adequate resting-state data variance. This may average out some of the fast-occurring variability effects; however, another study is currently analyzing the technical aspects of SliTICA in detail. The extended amount of information required new steps for visualization of the data and condensing of the results. One visualization issue is the splitting of DMN components into a few rather similar ones on the some occasions. Their relevance and behavior must be further analyzed because this study focused on just one DMN component at a time in order not to be too complex. Also, the autocorrelation structure of the time domain spatial similarity measures of overlapping time windows will be more thoroughly investigated in the future, as more information on the spatial variance of activity in time emerges.

The spatio-temporal accuracy of the SliTICA approach was measured in detecting a known BOLD glitch artifact of one data set. The measurements suggest that the SliTICA approach is spatially and temporally robust in detecting the artifact as a statistically independent signal source. In addition, the relatively stable exponential decays and, more important, the stable explained variance of the successive DMN maps suggest that the algorithm itself is stable, especially because the dimensionality of the data remains stable from window to window, based on model order estimates. Because the information on the combined spatio-temporal variability of brain activity is just starting to emerge, a plausible artificial data model for realistic testing of the SliTICA approach for resting-state brain activity is not yet possible. Another study is exploring the temporal accuracy limits of the window length for such ICA variables as model order; this study is also obtaining more information on spatio-temporal variability of resting-state source data. In addition, more robust computer-based identification methods for successive

SliTICA components are needed to speed up the relatively time consuming and subjective visual verification. The establishment of individual SliTICA image thresholds requires more thorough statistical modeling of the partly overlapping data sets in SliTICA. However, at this stage the development of a valid model for spatiotemporal brain activity variance is just beginning.

Conclusion

Sliding-window ICA reveals marked spatial variance within the DMN over time. The spatial similarity of the DMN presents low-frequency fluctuations that show 1/f behavior compared with the whole time measurement. The commonly used whole time series spatial ICA is separated from temporally sparse events rather than comprehensive mapping of the network. Importantly, the temporal sparseness can be reduced by forcing ICA to detect DMN maps from short time windows. The detected spatial edges and relative strengths of activity within voxels of the DMN alter markedly over time. Of note, the incidental DMN connectivity to other areas seems to grow centrifugally from the DMN core in a manner similar to that of task activation repeatability. The lower the incidence threshold, the more widespread activity is mapped. The SliTICA approach can be used to produce a more comprehensive picture of the functional integrity of resting-state networks, such as the default mode. This may augment individual-level measurements and diagnostics.

Acknowledgments

Academy of Finland grants 111711 and 123772, a Finnish Medical Foundation grant, and a Finnish Neurological Association grant contributed to this study. Comments from Christian Beckmann are cordially acknowledged. Nick Hayward of Scientific English, United Kingdom, is thanked for swift English proofreading.

Author Disclosure Statement

None of the authors have competing financial interests.

References

Abou-Elseoud A, Starck T, Remes J, Nikkinen J, Tervonen O, Kiviniemi V. 2010. The effect of model order selection in group PICA. Hum Brain Mapp. 31:1207–1216.

Achard S, Salvador R, Whitcher B, Suckling J, Bullmore E. 2006. A resilient, low-frequency, small-world human brain functional network with highly connected association cortical hubs. J Neurosci. 26:63–72.

Beckmann CF, DeLuca M, Devlin JT, Smith SM. 2005. Investigations into resting-state connectivity using independent component analysis. Philos Trans R Soc Lond B Biol Sci 360: 1001–1013.

Beckmann CF, Smith SM. 2004. Probabilistic independent component analysis for functional magnetic resonance. IEEE Trans Med Imaging 23:137–152.

Bellec P, Rosa-Neto P, Lyttelton OC, Benali H, Evans AC. 2010. Multi-level bootstrap analysis of stable clusters in resting-state fMRI. Neuroimage 51:1126–1139.

Birn RM, Saad ZS, Bandettini PA. 2001. Spatial heterogeneity of the nonlinear dynamics in the FMRI BOLD response. Neuroimage 14:817–826.

Biswal B, Yetkin FZ, Haughton VM, Hyde JS. 1995. Functional connectivity in the motor cortex of resting human brain using echo-planar MRI. Magn Reson Med 34:537–541.

Biswal BB, Mennes M, Zuo XN, Gohel S, Kelly C, Smith SM, et al. 2010. Toward discovery science of human brain function. Proc Natl Acad Sci U S A 107:4734–4739.

Buckner RL, Andrews-Hanna JR, Schacter DL. 2008. The brain's default network: anatomy, function, and relevance to disease. Ann N Y Acad Sci 1124:1–38.

Calhoun VD, Adali T, Pearlson G, Pekar J. 2001. A method for making group inferences from fMRI data using independent component analysis. Hum Brain Mapp 14:140–151.

Chang C, Glover GH. 2010. Time-frequency dynamics of resting-state brain connectivity measured with fMRI. Neuroimage. 50:81–98.

Cohen AL, Fair DA, Dosenbach NU, Miezin FM, Dierker D, Van Essen DC, et al. 2008. Defining functional areas in individual human brains using resting functional connectivity MRI. Neuroimage 41:45–57.

Damoiseaux JS, Rombouts SA, Barkhof F, Scheltens P, Stam CJ, Smith SM, Beckmann CF. 2006. Consistent resting-state networks across healthy subjects. Proc Natl Acad Sci U S A 103:13848–13853.

Daubechies I, Roussos E, Takerkart S, Benharrosh M, Golden C, D'Ardenne K, et al . 2009. Independent component analysis for brain fMRI does not select for independence. Proc Natl Acad Sci U S A 106:10415–10422.

Esposito F, Seifritz E, Formisano E, Morrone R, Scarabino T, Tedeschi G, et al. 2003. Real-time independent component analysis of fMRI time-series. Neuroimage. 20:2209–2224.

Fernandez G, Specht K, Weis S, Tendolkar I, Reuber M, Fell J, et al. 2003. Intrasubject reproducibility of presurgical language lateralization and mapping using fMRI. Neurology 60:969–975.

Fox MD, Greicius M. Clinical applications of resting state functional connectivity. 2010. Front Syst Neurosci. 4:19.

Fox MD, Raichle ME. 2007. Spontaneous fluctuations in brain activity observed with functional magnetic resonance imaging. Nat Rev Neurosci 8:700–711.

Fox MD, Snyder AZ, Vincent JL, Corbetta M, Van Essen DC, Raichle ME. 2005. The human brain is intrinsically organized into dynamic, anticorrelated functional networks. Proc Natl Acad Sci U S A 102:9673–9678.

Friston KJ. 2011. Functional and effective connectivity: a review. Brain Connectivity. 1:13–36.

Greicius MD, Srivastava G, Reiss AL, Menon V. 2004. Default-mode network activity distinguishes Alzheimer's disease from healthy aging: evidence from functional MRI. Proc Natl Acad Sci U S A 101:4637–4642.

Greicius M. Resting-state functional connectivity in neuropsychiatric disorders. 2008. Curr Opin Neurol 21:424–340.

Hyvärinen A. 1999. Fast and robust fixed-point algorithms for independent component analysis. IEEE Trans Neural Networks 10:626–634.

Jenkinson M, Bannister P, Brady M, Smith S. 2002. Improved optimization for the robust and accurate linear registration and motion correction of brain images. Neuroimage 17:825–841.

Kannurpatti SS, Biswal BB. 2008. Detection and scaling of task-induced fMRI-BOLD response using resting state fluctuations. Neuroimage 40:1567–1574.

Kannurpatti SS, Motes MA, Rypma B, Biswal BB. 2011. Increasing measurement accuracy of age-related BOLD signal change: minimizing vascular contributions by resting-state-fluctuation-of-amplitude scaling. Hum Brain Mapp 32:1125–1140.

Karvanen J, Theis F. Spatial ICA of fMRI Data in Time Windows. In: AIP Conference Proceedings, Garching, Germany, 2004, pp. 312–319.

Kiviniemi V, Kantola JH, Jauhiainen J, Hyvarinen A, Tervonen O. 2003. Independent component analysis of nondeterministic fMRI signal sources. Neuroimage 19:253–260.

Kiviniemi V, Starck T, Remes J, Long X, Nikkinen J, Haapea M, et al. 2009. Functional segmentation of the brain cortex using high model order group PICA. Hum Brain Mapp 30:3865–3886.

Long XY, Zuo XN, Kiviniemi V, Yang Y, Zou QH, Zhu CZ, et al. 2008. Default mode network as revealed with multiple methods for resting-state functional MRI analysis. J Neurosci Methods. 171:349–355.

Marellec G, Fransson P. 2011. Assessing the influence of different ROI selection strategies on functional connectivity analyses of fMRI data acquired during steady-state conditions. PLoS ONE 6:e14788.

McKeown MJ, Makeig S, Brown GG, Jung TP, Kindermann SS, Bell AJ, Sejnowski TJ. 1998. Analysis of fMRI data by blind separation into independent spatial components. Hum Brain Mapp 6:160–188.

Mennes M, Kelly C, Zuo XN, Di Martino A, Biswal BB, Castellanos FX, Milham MP. 2010. Inter-individual differences in resting-state functional connectivity predict task-induced BOLD activity. Neuroimage 50:1690–1701.

Mennes M, Zuo XN, Kelly C, Di Martino A, Zang YF, Biswal B, et al. 2011. Linking inter-individual differences in neural activation and behavior to intrinsic brain dynamics. Neuroimage 54:2950–2959.

Neumann J, Lohmann G, Zysset S, von Cramon DY. 2003. Within-subject variability of BOLD response dynamics. Neuroimage 19:784–796.

Raichle ME, MacLeod AM, Snyder AZ, Powers WJ, Gusnard DA, Shulman GL. 2001. A default mode of brain function. Proc Natl Acad Sci U S A 98:676–682.

Rombouts SA, Barkhof F, Hoogenraad FG, Sprenger M, Scheltens P. Within-subject reproducibility of visual activation patterns with functional magnetic resonance imaging using multislice echo planar imaging. 1998. Magn Reson Imaging 16:105–113

Saad ZS, Ropella KM, DeYoe EA, Bandettini PA. 2003. The spatial extent of the BOLD response. Neuroimage 19:132–144.

Salli E, Korvenoja A, Visa A, Katila T, Aronen HJ. 2001. Reproducibility of fMRI: effect of the use of contextual information. Neuroimage 13:459–471.

Smith SM. 2002. Fast robust automated brain extraction. Hum Brain Mapp 17:143–155.

Smith SM, Fox PT, Miller KL, Glahn DC, Fox PM, Mackay CE, et al. 2009. Correspondence of the brain's functional architecture during activation and rest. Proc Natl Acad Sci U S A 106:13040–13045.

Smith SM, Miller KL, Salimi-Khorshidi G, Webster M, Beckmann CF, Nichols TE, et al. 2011. Network modelling methods for FMRI. Neuroimage 54:875–891.

Tjandra T, Brooks JC, Figueiredo P, Wise R, Matthews PM, Tracey I. 2005. Quantitative assessment of the reproducibility of functional activation measured with BOLD and MR perfusion imaging: implications for clinical trial design. Neuroimage 27:393–401.

van Gelderen P, C WHW, de Zwart JA, Cohen L, Hallett M, Duyn JH. 2005. Resolution and reproducibility of BOLD and perfusion functional MRI at 3.0 Tesla. Magn Reson Med 54:569–576.

Yan X, Kelley S, Goldberg M, Biswal BB. 2011. Detecting overlapped functional clusters in resting state fMRI with Connected Iterative Scan: a graph theory based clustering algorithm. J Neurosci Methods 199:108–118.

Yoo SS, Wei X, Dickey CC, Guttmann CR, Panych LP. 2005.Long-term reproducibility analysis of fMRI using hand motor task. Int J Neurosci 115:55–77.

Address correspondence to:
Vesa Kiviniemi
Diagnostic Radiology
P. O. Box 50
90029 OYS
Finland

E-mail: vesa.kiviniemi@oulu.fi